Journal of Materials Chemistry

Dynamic Article Links

Cite this: *J. Mater. Chem.*, 2012, **22**, 14001

www.rsc.org/materials

PAPER

Fabrication of MMO–TiO_2 one-dimensional photonic crystal and its application as a colorimetric sensor†

Yibo Dou, Jingbin Han, Tengli Wang, Min Wei,* David G. Evans and Xue Duan

Received 13th March 2012, Accepted 23rd May 2012
DOI: 10.1039/c2jm31560b

This work reports the fabrication of porous mixed metal oxide (MMO)–TiO_2 one-dimensional photonic crystals (1DPCs), which can be used as a colorimetric sensor for the detection and measurement of volatile organic compounds (VOCs) and relative humidity (RH). The 1DPCs were prepared *via* the alternate deposition of titania and layered double hydroxide (LDH) by the spin-coating technique followed by calcination (which induces the phase transformation of LDH to MMO material). A photonic stop band (PSB) of MMO–TiO_2 1DPCs was obtained, which can be tuned throughout the whole visible light region by changing the thickness of either of the composing slabs, as a result of the sufficiently high refractive index contrast between TiO_2 and MMO. The 1DPC film as a colorimetric sensor shows significant color variation towards VOCs or RH, due to the change of refractive index induced by the adsorption of volatile gas or water molecule in the mesopores of the MMO–TiO_2 structure. In addition, the sensor displays high sensitivity, good stability and reproducibility. Therefore, this work provides a feasible method for the fabrication of 1DPCs based on porous MMO–TiO_2 films, which have potential applications as portable, recyclable and visually readable colorimetric sensors.

1. Introduction

One-dimensional photonic crystals (1DPCs) are multilayer stacks composed of a periodic structure of high- and low-refractive-index materials, giving rise to high reflectivity at the position of the photonic stop band (PSB). If the PSB arises in the visible region of the electromagnetic spectrum, the 1DPCs present have a bright color, which is also referred to as the "structural color".[1–3] 1DPCs have generated significant attention and enthusiasm because they exhibit a material-specific response profile to external stimuli, which can be used as distributed feedback lasers,[4] displays[5] and sensors.[6] Recently, porous 1DPCs have attracted considerable interest in the field of chemical and bio-sensing, due to the change in the optical response caused by the presence of target species.[7] The most effective way to create nanoporous 1DPCs is to alternately deposit porous films with different refractive indexes. For instance, TiO_2 and SiO_2 are one of the preferred pairs for base materials to build such structures, owing to the large contrast of dielectric constant between them.[8,9] Although nanoporous TiO_2–SiO_2 1DPCs have been reported *via* the sol–gel route, the stack fabrication process was generally extremely time consuming and harsh conditions were required.[10] Moreover, the random-close packing of nanoparticles restricts the achievable porosity and consequently the optical sensitivity of obtained 1DPCs was normally unsatisfactory. Therefore, it is highly essential to explore new materials or approaches to obtain 1DPCs with a largely enhanced optical response.

Reliable sensors for detecting volatile organic compounds (VOCs) or monitoring relative humidity (RH) play an important role in ensuring appropriate conditions in industrial, agricultural and medical fields.[11,12] Several sensors for VOCs and RH based on metal oxides,[13] silicon[14] and ceramics[15] have been commercialized and widely applied and which generally work through complicated signal-receive systems and have to be driven by external power. This to some extent restricts their practical application. Compared with traditional devices, the sensing platform based on photonic crystals has the advantages of low cost, easy portability and visual readability, which requires no specific apparatus for operation and no power consumption.[16,17] However, inorganic materials-based 1DPCs normally display little shift of PSB by ex-stimuli and therefore low resolution among various target species.[18] As an important supplement, polymer-based 1DPCs were successfully prepared by the self-assembly of block copolymers, and their optical properties could be largely tuned by swelling the polymer in the presence of water or organic solvents.[19] Nevertheless, they suffer from the complicated synthesis of specific block polymers, poor stability

State Key Laboratory of Chemical Resource Engineering, Beijing University of Chemical Technology, Beijing, 100029, China. E-mail: weimin@mail.buct.edu.cn; Fax: +86-10-64425385; Tel: +86-10-64412131

† Electronic supplementary information (ESI) available: Powder XRD patterns (Fig. S1); SEM images (Fig. S2); film XRD patterns (Fig. S3); the experimental and fitted curves (Fig. S4); film tested for adhesion (Fig. S5); optical spectra and digital photographs (Fig. S6); the change of water-contact angle (Fig. S7). See DOI: 10.1039/c2jm31560b

as well as a complex preparation process.[20,21] Therefore, it is still a challenge to achieve environmentally responsive 1DPCs which can resolve the problems mentioned above and simultaneously exhibit high sensitivity, good reversibility and stability in the detection of VOCs or humidity.

Layered double hydroxides (LDHs) or hydrotalcites, are layered anionic clays generally expressed by the formula $[M^{2+}_{1-x}M^{3+}_{x}(OH)_2](A^{n-})_{x/n}\cdot mH_2O$, where M^{2+} and M^{3+} are metal cations and A^{n-} is a charge-compensating anion.[22,23] Calcination of LDHs at moderate temperatures leads to the formation of mixed metal oxides (MMOs) with a porous structure, which have attracted considerable interest in view of their versatility and functionality in a wide range of applications in catalysts, ion exchangers, adsorbents for environmental remediation and carriers for biological materials.[24,25] These unique features therefore inspired us to fabricate a new 1DPC based on the incorporation of MMO material and titania owing to their large contrast of dielectric constant. In contrast to the compact inorganic or polymer-based 1DPCs, the MMO–TiO_2 1DPCs offer several advantages: firstly, a porous structure and large specific surface area of MMO materials provide 1DPCs with an accessible space for target species, which enlarges the PSB shift in a broad scope and thus enhances the sensitivity accordingly; secondly, this inorganic–inorganic architecture would improve the stability (optical, thermal and mechanical) and environmental compatibility of 1DPC sensors.

In this work, we reported a porous MMO–TiO_2 1DPC fabricated by spin-coating multilayer films of TiO_2 and LDH nanoparticles alternately followed by subsequent calcination, which serves as a colorimetric sensor for the detection of VOCs or RH (Scheme 1). The 1DPCs display brilliant color in the whole visible light region *via* thickness modulation of either composing slab owing to the high refractive index contrast between titania (1.96) and MMO (1.28). The MMO–TiO_2 1DPCs show a colorimetric response towards several VOCs or RH, as a result of the change in refractive index contrast originating from the adsorption of VOC or water molecules in the nanopores of the MMO slab. Furthermore, a quantitative measurement for a specific VOC (for instance, acetone in the range 0–0.0387 mol l^{-1}) as well as for RH (in the range 5–85%) can be successfully performed accompanied by a distinct color change of the 1DPC. In addition, the porous 1DPC sensors display a good reversibility and high stability. Therefore, this work provides a facile and cost-effective strategy for the fabrication of MMO-based 1DPCs, which can be potentially used in environmental monitoring and chemical/biochemical detection.

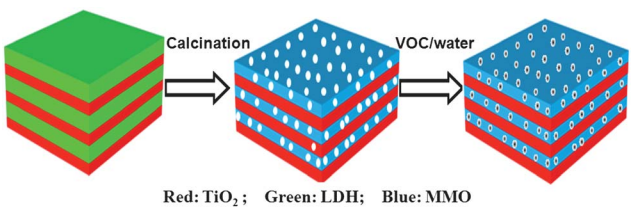

Scheme 1 Schematic illustration of the MMO–TiO_2 1DPC for VOC or humidity detection.

2. Experimental section

2.1. Materials

The $Ti(OEt)_4$ and P123 (PEO–PPO–PEO) were purchased from Sigma-Aldrich Company. The following chemicals: HCl, NaOH, $Mg(NO_3)_2\cdot 6H_2O$, $Al(NO_3)_3\cdot 9H_2O$, BuOH, H_2O_2, H_2SO_4, NaCl, KCl, ether, acetone, methanal and toluene were analytical grade and used without further purification. Deionized water was used in all the experimental processes.

2.2. Synthesis of LDH and TiO_2 colloidal suspensions

Colloidal LDH suspension was prepared according to the separate nucleation and aging steps (SNAS) method reported by our group.[26] Typically, 100 ml of solution A ($Mg(NO_3)_2\cdot 6H_2O$, 0.2 M and $Al(NO_3)_3\cdot 9H_2O$, 0.1 M) and 400 ml of solution B (NaOH, 0.15 M) were simultaneously added to a colloid mill with a rotor speed of 3000 rpm and mixed for 1 min. The resulting LDH slurry was obtained *via* centrifugation and washed twice with deionized water and then dispersed in 400 ml of deionized water. This aqueous suspension was transferred into a stainless steel autoclave with a Teflon® lining. After hydrothermal treatment at 110 °C for 24 h, a stable homogeneous LDH suspension with narrow size distribution was obtained. Titania nanoparticles (diameter 5–10 nm) were synthesized based on the reported method:[27] P123 (1.3 g) was firstly dissolved in BuOH (14.8 ml) and then added to a solution of $Ti(OEt)_4$ (3.8 ml) and HCl (2.7 ml, 36%) under vigorous stirring. The resulting clear sol was stirred for 3 h at room temperature and filtered (0.2 mm) prior to spin-coating.

2.3. Fabrication of MMO–TiO_2 multilayer films

Multilayer films of LDH–TiO_2 were fabricated by applying the spin-coating procedure. To increase the surface hydrophilicity of silicon wafers for the aqueous LDH suspension, the wafers were pre-cleaned with Piranha (H_2SO_4 : H_2O_2, 3 : 1) solution for 30 min. The LDH suspension (60 s per cycle, 2500 rpm) and TiO_2 suspension (10 s per cycle, 4500 rpm) were spin-coated onto a silicon wafer alternatively. The films were baked at 60 °C for 10 min after each spin-coating process. Subsequently, a series of these operations for LDH and TiO_2 were repeated n times to obtain multilayer films of $(LDH–TiO_2)_n$. Finally, the substrates coated with $(LDH–TiO_2)_n$ films were annealed at 450 °C for 3 h to produce $(MMO–TiO_2)_n$ 1DPCs with a nanoporous structure.

2.4. Reflection measurements

The sensing experiment was carried out in a sealed environment. The ether, acetone, methanal and toluene were placed in a sealed quartz chamber respectively and stored overnight, so as to obtain the saturated vapor of the VOCs. The various concentrations of acetone vapor can be obtained by mixing ionic liquid and acetone with different ratios and were stored in a sealed quartz chamber for 12 h. Humidity-controlled solutions of 96% H_2SO_4, 54% H_2SO_4, saturated $Mg(NO_3)_2$, saturated NaCl and saturated KCl were respectively placed in a sealed quartz chamber at 25 °C for 24 h, which achieved different constant relative humidities (RH): 5%, 30%, 54%, 75% and 85%.[28] Subsequently, the

MMO–TiO_2 film was placed inside the sealed quartz chambers with VOCs or water vapor for 5 min and the corresponding reflection spectrum was recorded by the UV-vis spectrometer.

2.5. Characterization techniques

Powder X-ray diffraction (XRD) patterns of the samples were collected using a Shimadzu XRD-6000 diffractometer under the following conditions: 40 kV, 30 mA, graphite filtered Cu Kα radiation ($\lambda = 0.1542$ nm). The determination of the layer thickness, refractive index and porosity of the films was carried out using a spectroscopic ellipsometer (Angstrom Advanced Inc. PHE-102) at an incident angle of 70° within the spectral range of 300–800 nm. The modeling and fitting of the ellipsometric spectra were performed using the software provided by the manufacturer. Scanning electron microscopy (SEM) images were obtained on a Zeiss Supra 55 field emission scanning electron microscope with an EDX attachment. Atomic force microscopy (AFM) images were collected using a NanoScope IIIa AFM from Veeco Instruments in the tapping-mode in air. The measurement of the reflectance spectra of the 1DPC was conducted using a dual-channel spectrometer (Beijing Purkinje General, TU-1901). The CIE 2000 color coordinates were determined using a Photo Research PR-650 Spectra Scan colorimeter with the detector vertical to the surface of the MMO–TiO_2 film. The static water contact angles of 1DPCs were measured using a sessile drop at three different points of each film sample using a commercial drop shape analysis system (DSA100, KRüSS GmbH, Germany) at ambient temperature. The volume of water droplets used for the measurements was 2 μl.

3. Result and discussion

3.1. Preparation and characterization of 1DPCs

The XRD patterns of the MgAl–LDH and titania are shown in Fig. S1A and S1B†, which can be respectively indexed to a rhombohedral NO_3-containing LDH with 2θ 10.6° (d_{003} = 8.34 Å) and anatase titania 2θ 25.4° (d_{101} = 3.49 Å). No other crystalline phase is detected, indicating the LDH and titania were successfully prepared with high purity. The SEM images of Fig. S2A and S2B† reveal that the as-prepared LDH and TiO_2 nanoparticles are of high quality in terms of size and uniformity, with particle size of 45–55 nm and 5–10 nm, respectively. The obtained LDH–TiO_2 film prepared by a spin-coating method displays superimposed reflections of the LDH and TiO_2 phases (Fig. S3†, curve a). Calcination at 450 °C gives rise to the disappearance of the LDH reflections and the appearance of the 200 and 220 reflections were attributed to a MMO phase (Fig. S3†, curve b), which indicates the phase transformation from LDH to MMO during the calcination process. The effective refractive indexes of MMO and titania measured by spectroscopic ellipsometry are 1.28 and 1.96, respectively (see details in the ESI, Fig. S4†).

The sufficiently high refractive index contrast between the two components is beneficial in fabricating 1DPCs with high reflectivity.

In order to evaluate the surface and inter-stack roughness, which strongly influence the optical performance of 1DPCs, the surface morphology of the MMO–TiO_2 film was investigated by SEM and AFM. A typical top-view SEM image for a one-bilayer MMO–TiO_2 film with the MMO slab as the terminating layer (Fig. 1A) shows a continuous and uniform surface. The EDX spectrum (Fig. 1B) indicates the presence of the MgAl–MMO and TiO_2 components. The side view SEM image (Fig. 1C) illustrates a clear interface between the MMO and TiO_2 layers, with a thickness of ~70 and ~76 nm respectively for the two slabs. The AFM topographical image (500 nm × 500 nm, Fig. 1D) gives the morphology and roughness information of the one-bilayer stack, from which it can be seen that the film surface is relatively smooth with a root-mean square roughness of 18.57 nm. Furthermore, no delamination or peeling occurred on cross-cutting the film surface, indicating a strong adhesion of the film to the substrate (Fig. S5†).

The porous 1DPCs composed of alternate layers of TiO_2 and MMO slab were realized using a spin-coating technique and subsequent calcination, which present brilliant colored reflections when their PSB falls into the visible region of the spectrum (Fig. 2). The first-order reflected wavelength of a structure with periodic index profile can be predicted by Bragg's law:[29]

$$\lambda_{max} = 2(n_L d_L + n_H d_H) \quad (1)$$

where λ_{max} is the first-order reflected wavelength and n and d are the refractive index and thickness of the low-index regions (L) and high-index regions (H) in the film, respectively. Eqn (1) shows that the wavelength of maximum reflectance depends on the optical thickness (product of thickness and refractive index) of the two stacks. Therefore, the film color can be changed by varying the thickness of either slab. Firstly, we increased the thickness of the TiO_2 layer from 76 to 92 and 127 nm with a constant thickness of the MMO layer (70 nm). As shown in Fig. 2A, the corresponding PSB position of the three (MMO–TiO_2)$_n$ (n = 6) 1DPCs occurs at 449 nm, 532 nm and 690 nm respectively, and the PSB shift can also be visually verified by the accompanying color change from violet to green and then to pink (Fig. 2B). In addition, the thickness of the MMO layer can also

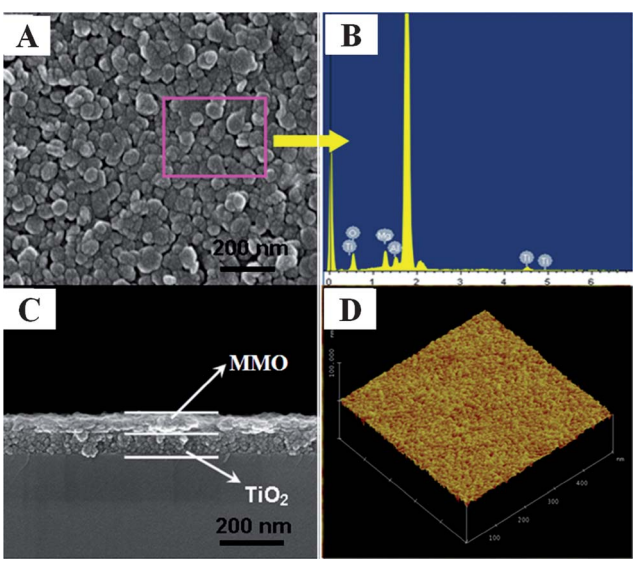

Fig. 1 (A) SEM image, (B) EDX spectrum, (C) cross sectional view and (D) AFM image of the (MMO–TiO_2)$_n$ (n = 1) film.

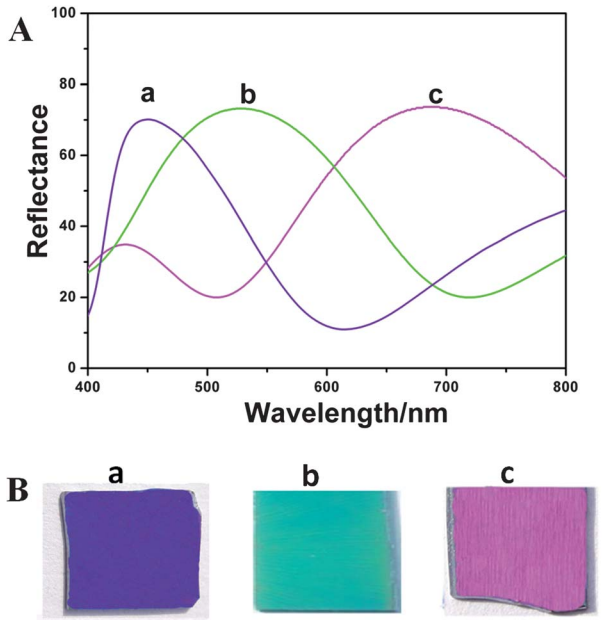

Fig. 2 (A) Optical spectra and (B) digital photographs showing full visible range colors by thickness modulation of three 1DPC samples $(MMO–TiO_2)_n$ ($n = 6$) (the thickness of MMO is constant at 70 nm and the thickness of TiO_2 are 76, 92 and 127 nm for (a), (b) and (c) respectively).

be controlled over a wide range, which induces the tunability of the stop band likewise across the whole visible range (Fig. S6†). The results above demonstrate that the color of the 1DPC can be varied in the entire visible range *via* changing the optical thickness of either of the stacks, as expected from eqn (1).

3.2. Colorimetric response of 1DPCs towards VOCs

The colorimetric response of the 1DPCs towards VOCs was studied by monitoring the UV-vis reflectance spectra. Fig. 3A displays the reflective spectra of the $(MMO–TiO_2)_6$ film in different environments, from which a significant red shift of PSB was observed as the 1DPC was immersed in various VOCs. The PSB of the $(MMO–TiO_2)_6$ film moves from 449 nm (in air) to 496 nm (in ether), 499 nm (in acetone), 506 nm (in methanal) and 515 nm (in toluene). The color coordinate of the 1DPC (Fig. 3B) also changes from violet (CIE: (0.241, 0.079)) to light blue (CIE: (0.117, 0.186)), blue (CIE: (0.114, 0.266)), blue-green (CIE: (0.101, 0.351)) and finally to green (CIE: (0.118, 0.449)). Photographs of the 1DPCs in air and various VOCs provide a visual verification of the color variation (Fig. 3C). The response of 1DPCs depending on the refractive index of the analyte was further investigated. As shown in Fig. 4, the reflectance maximum of three 1DPCs with different bilayers ($(MMO–TiO_2)_2$, $(MMO–TiO_2)_4$, $(MMO–TiO_2)_6$ respectively) exhibits a linear enhancement with the increase of refractive index of VOCs (The refractive indices of air, ether, acetone, methanal and toluene are 1.000, 1.353, 1.359, 1.375 and 1.496, respectively). The results demonstrate the higher the refractive index of analyte, the larger the shift of PSB. In addition, the bilayer number of the 1DPCs imposes a great influence on the sensitivity. The sensitivity ($\Delta\lambda/\Delta n$) of the $(MMO–TiO_2)_n$ films increases from 32 ($n = 2$) to 128 ($n = 6$), demonstrating a higher sensitivity towards VOCs compared with the conventional TiO_2-based 1DPCs.[9a,10] However, further increase of n results in nonuniformity of the 1DPC and in turn decreases its sensitivity. Therefore, $n = 6$ was chosen as the optimal bilayer number in this work.

Accurate information about the concentration of VOCs is generally required in practical application, as a result the optical response of the 1DPC towards specific VOC (such as acetone vapor) with different concentration was also measured. As shown in Fig. 5A, the PSB of $(MMO–TiO_2)_6$ 1DPC shifts to a longer wavelength upon increasing the concentration of acetone vapor from 0 to 0.0387 mol l^{-1}. The adsorption of acetone vapor results in an increase of the average refractive index of the 1DPC and the PSB shifts correspondingly. In addition, a linear increase of $\Delta\lambda$ as a function of acetone concentration (0–0.0387 mol l^{-1}) was observed (Fig. 5B) with a regression equation: $\Delta\lambda$ (nm) = 1.89 + 1.27 × 10^3 c (mol L^{-1}), $r^2 = 0.997$. The corresponding color coordinate (Fig. 5C) changes gradually from violet (CIE: (0.241, 0.079)) to blue (CIE: (0.119, 0.264)) upon increasing the concentration of acetone vapor, which was further visually observed in Fig. 5D. The results above indicate that the MMO–TiO_2 1DPC can be used as a visually readable sensor for the detection and measurement of VOCs.

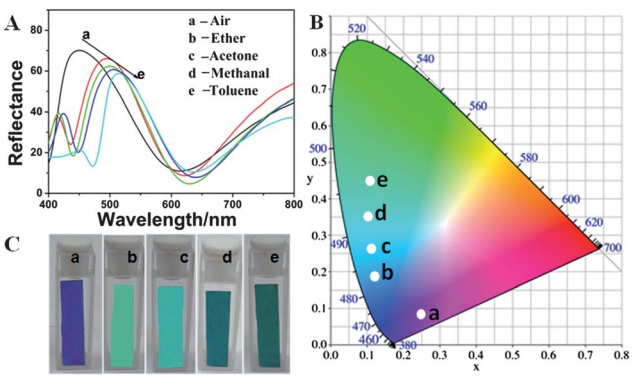

Fig. 3 (A) Reflectance spectra, (B) color coordinates and (C) photographs of the $(MMO–TiO_2)_6$ 1DPC in air (a) and various VOCs: (b) ether, (c) acetone, (d) methanal and (e) toluene.

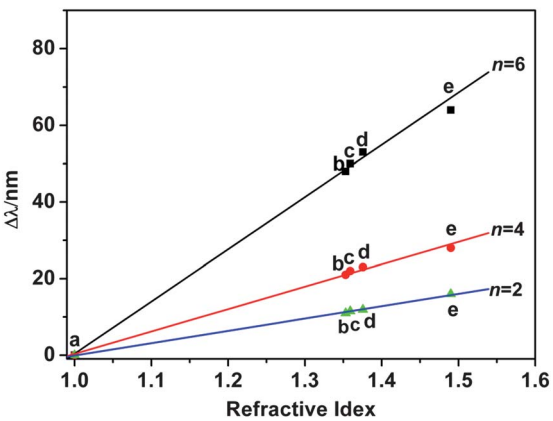

Fig. 4 The PSB shift ($\Delta\lambda$) for the $(MMO–TiO_2)_n$ films (n = 2, 4, 6 respectively) as a function of refractive index of analyte: (a) air, (b) ether, (c) acetone, (d) methanal and (e) toluene.

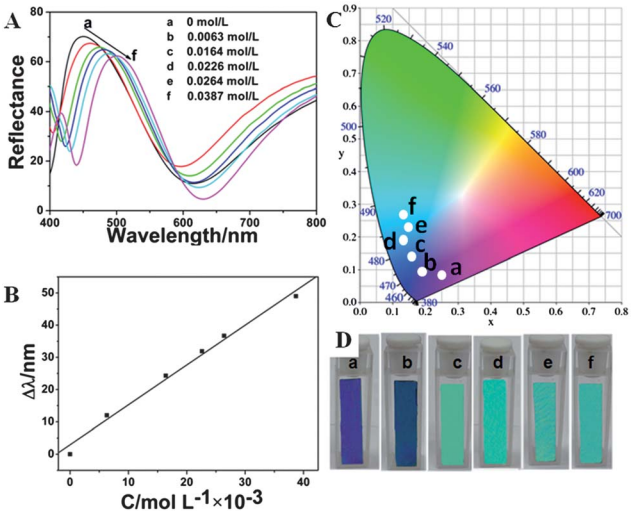

Fig. 5 Response of the $(MMO–TiO_2)_6$ 1DPC towards acetone vapor with various concentration: (A) reflectance spectra; (B) the linear correlation between PSB shift ($\Delta\lambda$) and acetone concentration; (C) the changes in color coordinates; (D) photographs of color variation (a–f: 0, 0.0063, 0.0164, 0.0226, 0.0264 and 0.0387 mol l^{-1}).

3.3. Colorimetric response of 1DPCs towards humidity

The response of the MMO–TiO_2 1DPCs towards different RH was further investigated. The obtained 1DPC is exposed in a closed container to various RH and its UV-vis reflectance spectra were recorded *in situ*. As the RH increases from 5% to 30%, 54%, 75% and 85%, the PSB position of the 1DPC shifts from 521 to 540, 569, 602 and 633 nm, respectively (Fig. 6A), with the maximum $\Delta\lambda$ of 112 nm. The relationship between the PSB position (λ) and RH can be fitted by the following exponential equation: λ (nm) = 488.4 + 29.4 $e^{(RH/54.5\%)}$, r^2 = 0.998 (Fig. 6D). The color coordinate measurements in Fig. 6B demonstrate that the color of 1DPC changes from bluish-green (CIE: (0.161, 0.353)) to yellow-green (CIE: (0.315, 0.499); CIE: (0.358, 0.519)) and then to orange (CIE: (0.501, 0.377)), finally to yellow-pink (CIE: (0.463, 0.283)). The corresponding photographs in Fig. 6C also illustrate the significant color variation of 1PDC under different RH conditions. This can be attributed to the adsorption of water molecules in the 1DPC pores and the resultant change of refractive indexes, which translates into a marked shift of the PSB position. Compared with traditional electric sensors, this MMO–TiO_2 1DPC as an optical sensor offers a more attractive way to detect a specific signal *via* color change, without using complex data collection systems and expensive display units. In addition, the facile fabrication approach and easy manipulation render the 1DPCs as a promising candidate for VOC or RH sensors with further potential applications.

The response sensitivity is another important parameter for evaluating the performance of a RH sensor. It was reported that the wettability of the TiO_2 surface can be promoted by UV illumination, which is favorable for the adsorption of water molecules.[30,31] Therefore, the influence of UV illumination on the senor sensitivity was also investigated. A response comparison of the 1DPC film before and after UV-illumination towards different RH are shown in Fig. 7, from which a larger PSB shift upon UV irradiation was observed. The enhanced RH response is attributed to the more superhydrophilic 1DPC surface, which was further confirmed by the contact angle measurements. The contact angle of the 1DPCs surface decreased from ~25° to ~0° upon UV irradiation (inset of Fig. 7), indicating a significant increase in the wettability. It has been reported that UV illumination of TiO_2 enhances surface hydrophility originating from photo-generated Ti^{3+} defect sites, which facilitates the dissociative adsorption of water and the formation of hydrophilic domains.[32] It can thus be concluded that the promoted wettability of the 1DPC surface renders the affinity between 1DPC and water-vapor accordingly, resulting in an enhanced sensitivity for distinguishing humidity. Moreover, the UV-illuminated humidity sensor shows a self-cleaning property (see details in Fig. S7†), which is potentially useful for practical applications.

3.4. Stability and reversibility of the 1DPC sensor

Taking into account the potential applications and long-term maintenance of a visual sensor, the stability and reversibility of MMO–TiO_2 1DPC was further studied. By immersing the

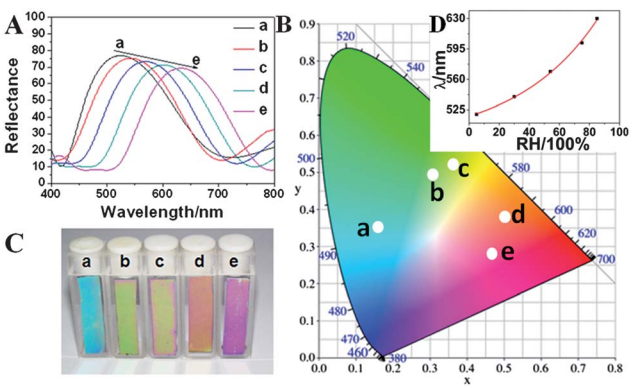

Fig. 6 Response of the $(MMO–TiO_2)_6$ 1DPC towards different relative humidity: (A) reflectance spectra; (B) the change in color coordinates; (C) photographs of color variation (a–e: 5%, 30%, 54%, 75% and 85%, respectively); (D) the exponential correlation between PSB position (λ) and RH.

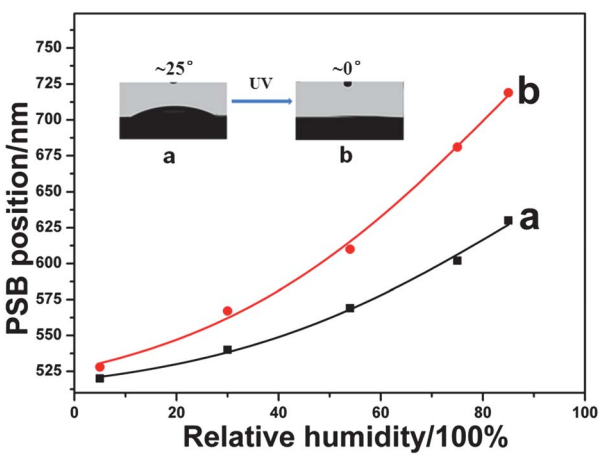

Fig. 7 The response of the $(MMO–TiO_2)_6$ 1DPC in various RH atmosphere before (a) and after (b) UV irradiation.

$(MMO–TiO_2)_6$ 1DPC sensor from air to ether/toluene vapor alternately, the PSB position shifts from 449 to 496/515 nm reversibly (Fig. 8A). The reversible performance can be readily repeated for 100 cycles with a relative standard deviation (RSD) of 0.53% (air), 0.71% (ether) and 0.85% (toluene), respectively. Fig. 8B displays that the PSB shift of the 1DPC film keeps almost constant for as long as 50 days, indicating the long-term stability of the VOCs sensor. As the 1DPC was alternately exposed to high (85%) and low (5%) RH condition for 10 cycles (Fig. 8C), the reversible PSB position shift illustrates good reproducibility of the RH sensor with the RSD of 0.72% (RH 5%) and 0.85% (RH 85%). To test the stability of the RH sensor, the 1DPC was measured at various RH for 50 days and the reflectance spectrum was recorded *in situ*. The results (Fig. 8D) show that no obvious signal drift was observed, which confirms its high stability. Therefore, the high reversibility, stability as well as good repeatability guarantee $MMO–TiO_2$ 1DPC serving as an optical sensor with prospective applications in VOCs or RH detection.

4. Conclusions

In summary, we have demonstrated a colorimetric sensor based on $MMO–TiO_2$ 1DPCs through a cost-effective spin-coating technique and subsequent calcination. The obtained 1DPCs exhibit a brilliant color which can be tuned in the whole visible light range by changing the thickness of either composing slab, originating from the shift of stop band. The $(MMO–TiO_2)_6$ 1DPC can be applied as a sensor for qualitative detection and quantitative measurement of various VOCs, owing to the change of the average refractive index by adsorption of organic molecules. Furthermore, the 1DPC shows fast response towards the variation of humidity, evidenced by a distinct color change as seen by the naked eye. In addition, the response behavior of the VOCs and RH sensor represents high reversibility, stability as well as good repeatability. Therefore, this work provides a visually readable colorimetric sensor based on porous $MMO–TiO_2$ 1DPCs, which can be potentially applied in environmental monitoring and chemical/biochemical sensing.

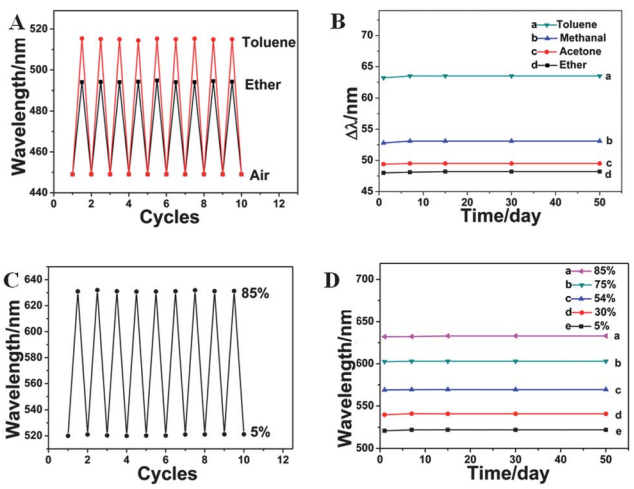

Fig. 8 The repeatability and stability of the $(MMO–TiO_2)_6$ 1DPC sensor: (A) optical response of the 1DPC in air, ether and toluene vapor alternately for 10 cycles; (B) the PSB shift ($\Delta\lambda$) of the 1DPC in VOCs for 50 days; (C) 10 cycles of 1DPC exposing in 5% and 85% RH alternately; (D) optical response of the 1DPC in various RH for 50 days.

Acknowledgements

This work was supported by the National Natural Science Foundation of China, the 973 Program (Grant no.: 2011CBA00504), the 111 Project (Grant no.: B07004), the Collaboration Project from the Beijing Education Committee and the Fundamental Research Funds for the Central Universities (Grant no.: ZY1215).

Notes and references

1 (*a*) N. Hidalgo, M. Calvo, M. Bellino, G. Soler-Illia and H. Míguez, *Adv. Funct. Mater.*, 2011, **21**, 2534; (*b*) L. Zhang, C. Baumanis, L. Robben, T. Kandiel and D. Bahnemann, *Small*, 2011, **7**, 2714.

2 (*a*) S. Takeda and P. Wiltzius, *Chem. Mater.*, 2006, **18**, 5643; (*b*) L. Zhang, R. Guo, M. Yang, X. Jiang and B. Liu, *Adv. Mater.*, 2007, **19**, 2988; (*c*) J. D. Joannopoulos, P. R. Villeneuve and S. H. Fan, *Nature*, 1997, **386**, 143; (*d*) P. Vukusic and J. R. Sambles, *Nature*, 2003, **424**, 852; (*e*) W. Hong, X. Hu, B. Zhao, F. Zhang and D. Zhang, *Adv. Mater.*, 2010, **22**, 5043.

3 (*a*) M. Kumoda, M. Watanabe and Y. Takeoka, *Langmuir*, 2006, **22**, 4403; (*b*) K. Matsubara, M. Watanabe and Y. Takeoka, *Angew. Chem., Int. Ed.*, 2007, **46**, 1688; (*c*) Y. Takeoka and M. Watanabe, *Langmuir*, 2003, **19**, 9104; (*d*) K. Ueno, K. Matsubara, M. Watanabe and Y. Takeoka, *Adv. Mater.*, 2007, **19**, 2807; (*e*) J. Texter, *C. R. Chim.*, 2003, **6**, 1425; (*f*) B. Lotsch, C. Knobbe and G. Ozin, *Small*, 2009, **5**, 1498.

4 D. Puzzo, F. Scotognella, M. Zavelani-Rossi, M. Sebastian, A. Lough, I. Manners, G. Lanzani, R. Tubino and G. Oizn, *Nano Lett.*, 2009, **9**, 4273.

5 J. Walish, Y. Kang, R. Mickiewicz and E. Thomas, *Adv. Mater.*, 2009, **21**, 3078.

6 X. Li, L. Peng, J. Cui, W. Li, C. Lin, D. Xu, T. Tian, G. Zhang, D. Zhang and G. Li, *Small*, 2012, **8**, 612.

7 Z. Wang, J. Zhang, J. Li, J. Xie, Y. Li, S. Liang, Z. Tian, C. Li, Z. Wang, T. Wang, H. Zhang and B. Yang, *J. Mater. Chem.*, 2011, **21**, 1264.

8 Z. Wu, D. Lee, M. Rubner and R. Cohen, *Small*, 2007, **3**, 1445.

9 (*a*) S. Colodrero, M. Ocaña, A. González-Elipe and H. Míguez, *Langmuir*, 2008, **24**, 9135; (*b*) L. Bonifacio, B. Lotsch, D. Puzzo, F. Scotognella and G. Ozin, *Adv. Mater.*, 2009, **21**, 1641.

10 S. Choi, M. Mamak, G. Freymann, N. Chopra and G. Ozin, *Nano Lett.*, 2006, **6**, 2456.

11 Z. Li, H. Zhang, W. Zheng, W. L. Wang, H. Huang, C. Wang, A. MacDiarmid and Y. Wei, *J. Am. Chem. Soc.*, 2008, **130**, 5036.

12 (*a*) Q. Kuang, C. Lao, Z. Wang, Z. Xie and L. Zheng, *J. Am. Chem. Soc.*, 2007, **129**, 6070; (*b*) L. Wallace, *Annu. Rev. Energy Environ.*, 2001, **26**, 269.

13 W. Qu, W. Wlodarski and J. Meyer, *Sens. Actuators, B*, 2000, **64**, 76.

14 Y. Xu, X. Li, J. He, X. Hu and H. Wang, *Sens. Actuators, B*, 2005, **105**, 219.

15 (*a*) K. Arshaka, K. Twomey and D. Egan, *Sensors*, 2002, **2**, 50; (*b*) V. Timar-Horvath, L. Juhasz, A. Vass-Varnai and G. Perlaky, *Microsyst. Technol.*, 2008, **14**, 1081.

16 P. Kurt, D. Banerjee, M. Rubner and R. Cohen, *J. Mater. Chem.*, 2009, **19**, 8920.

17 D. Puzzo, L. Bonifacio, J. Oreopoulos, C. Yip, I. Manners and G. Ozin, *J. Mater. Chem.*, 2009, **19**, 3500.

18 M. Fuertes, F. López-Alcaraz, M. Marchi, H. Troiani, V. Luca, H. Míguez and G. Soler-Illia, *Adv. Funct. Mater.*, 2007, **17**, 1247.

19 (*a*) Y. Kang, J. Walish, T. Gorishnyy and E. Thomas, *Nat. Mater.*, 2007, **6**, 957; (*b*) T. Kazmierczak, H. Song, A. Hiltner and E. Baer, *Macromol. Rapid Commun.*, 2007, **28**, 2210.

20 (*a*) R. Jakubiak, T. Bunning, R. Vaia, L. Natarajan and V. Tondiglia, *Adv. Mater.*, 2003, **15**, 241; (*b*) V. Hsiao, W. Kirkey, F. Chen, A. Cartwright, P. Prasad and T. Bunning, *Adv. Mater.*, 2005, **17**, 2211; (*c*) J. Shi, V. Hsiao, T. Walker and T. Huang, *Sens. Actuators, B*, 2008, **129**, 391.

21 (*a*) L. Zhai, A. Nolte, R. Cohen and M. Rubner, *Macromolecules*, 2004, **37**, 6113; (*b*) T. Kazmierczak, H. M. Song, A. Hiltner and E. Baer, *Macromol. Rapid Commun.*, 2007, **28**, 2210.
22 (*a*) B. Monteiro, S. Gago, F. A. A. Paz, R. Bilsborrow, I. S. Gonçalves and M. Pillinger, *Inorg. Chem.*, 2008, **47**, 8674; (*b*) G. R. Williams and D. O'Hare, *J. Mater. Chem.*, 2006, **16**, 3065; (*c*) D. Yan, J. Lu, J. Ma, S. Qin, M. Wei, D. G. Evans and X. Duan, *Angew. Chem., Int. Ed.*, 2011, **50**, 7037; (*d*) A. Illaik, C. Taviot-Guého, J. Lavis, S. Commereuc, V. Verney and F. Leroux, *Chem. Mater.*, 2008, **20**, 4854; (*e*) J. Y. Uan, J. K. Lin and Y. S. Yung, *J. Mater. Chem.*, 2010, **20**, 761; (*f*) A. M. Fogg, V. M. Green, H. G. Harvey and D. O'Hare, *Adv. Mater.*, 1999, **11**, 1466; (*g*) X. Hou and R. J. Kirkpatrick, *Inorg. Chem.*, 2001, **40**, 6397; (*h*) W. Shi, Y. Lin, S. He, Y. Zhao, C. Li, M. Wei, D. G. Evans and X. Duan, *J. Mater. Chem.*, 2011, **21**, 11116; (*i*) G. R. Williams, T. G. Dunbar, A. J. Beer, A. M. Fogg and D. O'Hare, *J. Mater. Chem.*, 2006, **16**, 1231; (*j*) F. Leroux and C. Taviot-Guého, *J. Mater. Chem.*, 2005, **15**, 3628; (*k*) W. Shi, S. He, M. Wei, D. G. Evans and X. Duan, *Adv. Funct. Mater.*, 2010, **20**, 3856.
23 (*a*) M. C. Richardson and P. S. Braterman, *J. Phys. Chem. C*, 2007, **111**, 4209; (*b*) J. W. Boclair and P. S. Braterman, *Chem. Mater.*, 1999, **11**, 298; (*c*) D. Yan, J. Lu, M. Wei, D. G. Evans and X. Duan, *J. Mater. Chem.*, 2011, **21**, 13128; (*d*) S. Gago, T. Costa, J. S. de Melo, I. S. Gonçalves and M. Pillinger, *J. Mater. Chem.*, 2008, **18**, 894; (*e*) S. Gago, M. Pillinger, R. A. S. Ferreira, L. D. Carlos, T. M. Santos and I. S. Gonçalves, *Chem. Mater.*, 2005, **17**, 5803; (*f*) X. Hou and R. J. Kirkpatrick, *Chem. Mater.*, 2002, **14**, 1195; (*g*) X. Zhao, F. Zhang, S. Xu, D. G. Evans and X. Duan, *Chem. Mater.*, 2010, **22**, 3933; (*h*) J. L. Gunjakar, T. W. Kim, H. N. Kim, I. Y. Kim and S. J. Hwang, *J. Am. Chem. Soc.*, 2011, **133**, 14998; (*i*) J. A. Kim, S. J. Hwang and J. H. Choy, *J. Nanosci. Nanotechnol.*, 2008, **8**, 5172.
24 J. Han, Y. Dou, M. Wei, D. G. Evans and X. Duan, *Angew. Chem., Int. Ed.*, 2010, **49**, 2171.
25 (*a*) F. Millange, R. I. Walton and D. O'Hare, *J. Mater. Chem.*, 2000, **10**, 1713; (*b*) J. Rocha, M. del Arco, V. Rives and M. A. Ulibarri, *J. Mater. Chem.*, 1999, **9**, 2499.
26 Y. Zhao, F. Li, R. Zhang, D. G. Evans and X. Duan, *Chem. Mater.*, 2002, **14**, 4286.
27 B. Lotsch and G. Ozin, *Adv. Mater.*, 2008, **20**, 4079.
28 J. Han, F. Fan, C. Xu, S. Lin, M. Wei, X. Duan and Z. L. Wang, *Nanotechnology*, 2010, **21**, 405203.
29 T. Alfrey, E. Gurnee and W. Schrenk, *Polym. Eng. Sci.*, 1969, **9**, 400.
30 R. Wang, K. Hashimoto and A. Fujishima, *Nature*, 1997, **388**, 431.
31 R. Wang, K. Hashimoto, A. Fujishima, M. Chikuni, E. Kojima, A. Kitamura, M. Shimohigoshi and T. Watanabe, *Adv. Mater.*, 1998, **10**, 135.
32 (*a*) R. Nakamura, K. Ueda and S. Sato, *Langmuir*, 2001, **17**, 2298; (*b*) A. Y. Nosaka, E. Kojima, T. Fujiwara, H. Yagi, H. Akutsu and Y. Nosaka, *J. Phys. Chem. B*, 2003, **107**, 12042; (*c*) C. Wang, H. Groenzin and M. J. Shultz, *Langmuir*, 2003, **19**, 7330; (*d*) J. M. White, J. Szanyi and M. A. Henderson, *J. Phys. Chem. B*, 2003, **107**, 9029; (*e*) N. Sakai, A. Fujishima, T. Watanabe and K. Hashimoto, *J. Phys. Chem. B*, 2003, **107**, 1028.